Atmos. Chem. Phys. Discuss., https://doi.org/10.5194/acp-2018-336
Manuscript under review for journal Atmos. Chem. Phys.
Discussion started: 16 May 2018

Atmospheric Chemistry and Physics Discussions

Low-level isoprene observed during summertime at a forested mountaintop site in southern China: implications for strong regional atmospheric oxidative capacity

Daocheng Gong[1,#], Hao Wang[1,2,#], Shenyang Zhang[1], Yu Wang[3], Shaw Liu[1], Hai Guo[3], Min Shao[1], Congrong He[2,4], Duohong Chen[5], Lingyan He[6], Lei Zhou[1], Lidia Morawska[2,4], Yuanhang Zhang[7], Boguang Wang[1,2,*]

[1]Institute for Environmental and Climate Research, Jinan University, Guangzhou 511443, China
[2]JNU–QUT Joint Laboratory for Air Quality Science and Management, Jinan University, Guangzhou 511443, China
[3]Air Quality Studies, Department of Civil and Environmental Engineering, The Hong Kong Polytechnic University, Hung Hom, Hong Kong
[4]International Laboratory for Air Quality and Health, Queensland University of Technology, GPO Box 2434, Brisbane, Queensland 4001, Australia
[5]State Environmental Protection Key Laboratory of Regional Air Quality Monitoring, Guangdong Environmental Monitoring Center, Guangzhou 510308, China
[6]Key Laboratory for Urban Habitat Environmental Science and Technology, School of Environment and Energy, Peking University Shenzhen Graduate School, Shenzhen 518055, China
[7]State Key Joint Laboratory of Environmental Simulation and Pollution Control, College of Environmental Sciences and Engineering, Peking University, Beijing 100871, China

[#] These authors contribute equally to this work

Correspondence to: Boguang Wang (tbongue@jnu.edu.cn)

Abstract

To investigate the atmospheric oxidizing capacity in certain polluted isoprene-rich environments, such as the forests surrounding megacities. Here we present online observations of isoprene and its first-stage oxidation products methyl vinyl ketone (MVK) and methacrolein (MACR) in summer 2016 at a remote, high-altitude mountain forest site (1,690 m a.s.l.) to the north of the air-polluted Pearl River Delta (PRD) region in southern China. The observed isoprene level was found to be significantly lower in comparison with other forest sites either in China or around the world, although the sampling site was surrounded with subtropical evergreen broad-leaved trees which are strong isoprene emitters. Also, high (MVK+MACR)/isoprene ratio was observed. Based on the observations, we hypothesized that the lower isoprene levels in the study forest might be attributable to a strong atmospheric oxidative capacity in relation to the elevated regional complex air pollution. High daytime OH and nighttime NO_3 radical concentrations estimated by using a photochemical box model incorporating Master Chemical Mechanism (PBM-MCM), as well as calculated short atmospheric reaction times of isoprene and long photochemical age, indicated that the isoprene was rapidly and fully oxidized at this aged atmospheric environment, which confirmed our hypothesis. The study suggests that the complex air pollution in the PRD region has significantly

elevated the background atmospheric oxidative capacity of the adjacent forests, and most likely does would probably affect the regional air quality and ecological environment in the long term. The feedback of forest ecosystems to the increasing atmospheric oxidation capacity warrants further studies.

Keywords: biogenic VOCs; isoprene; atmospheric oxidative capacity; Nanling Mountains; Pearl River Delta

1 Introduction

Isoprene is the most abundant non-methane volatile organic compound (NMVOC) in the atmosphere (Guenther et al., 2012). The reactive chemistry of isoprene affects the oxidation capacity of the troposphere and can contribute to the formation of ozone (O_3) and secondary organic aerosol (Claeys et al., 2004;Lelieveld et al., 2008). The biogenic sources from terrestrial vegetation contribute more than 90% of atmospheric isoprene, with the largest contribution from forests (Guenther et al., 2006).

Isoprene emissions from forests have been extensively studied over the past decades (Guenther et al., 1991). More recent work have expanded the focus from emissions to impacts on regional forest chemistry (Seco et al., 2011;Taraborrelli et al., 2012;Fuchs et al., 2013;Xu et al., 2015;Liu et al., 2016;Kleinman et al., 2016;Su et al., 2016;Gu et al., 2017;Schulze et al., 2017). These studies have greatly improved our understanding on oxidation process of isoprene, revealed current uncertainties associated with isoprene emission rates and degradation schemes, and highlighted the biogenic−anthropogenic interactions in certain polluted isoprene-rich environments, such as the forests surrounding megacities (Hofzumahaus et al., 2009;Rohrer et al., 2014).

After released into the troposphere, isoprene is rapidly removed mainly by oxidation of hydroxyl (OH) radical and nitrate (NO_3) radical. Ambient measurement in pristine forests (e.g. the Amazonian rainforest) found that high OH concentrations often occur under high-isoprene and low-NO_x ($NO_x \equiv NO+NO_2$, < 1 ppbv) conditions (Lelieveld et al., 2008;Rohrer et al., 2014). In those areas, OH regeneration contributes greatly to the oxidizing capacity of the atmosphere (Lelieveld et al., 2008;Fuchs et al., 2013). In addition, relatively high OH-recycling efficiency is not unique to pristine forests, it has been argued that above an isoprene emitting forest, at high concentration of pollutants, there may be important, but different OH-recycling mechanism (Hofzumahaus et al., 2009). Studies have also shown that small increases of NO concentration above the background level can lead to a large change in the air quality of the forest (Liu et al., 2016;Su et al., 2016).

Oxidation by OH radicals dominates daytime isoprene removal, and the oxidation is usually initiated by additional reaction of an OH across the double bond followed by fast reaction with oxygen (O_2). A population of hydroxyl-substituted isoprene peroxyl radicals (ISOPOO) are thereby produced (Orlando and Tyndall, 2012). The subsequent reactions of ISOPOO radicals proceed along several competing pathways (Jenkin et al., 2015). In polluted forest areas, the NO pathway likely dominates. The major products are NO_2, methyl vinyl ketone (MVK), and methacrolein (MACR).

Atmos. Chem. Phys. Discuss., https://doi.org/10.5194/acp-2018-336
Manuscript under review for journal Atmos. Chem. Phys.
Discussion started: 16 May 2018

The dominant night-time oxidant for isoprene is the NO_3 radical (Sobanski et al., 2016;Schulze et al., 2017;Edwards et al., 2017). NO_3 formed through the O_3 and NO_2 reaction can be abundant at night and react rapidly with isoprene (Brown et al., 2016;Millet et al., 2016). Production of NO_3 directly depends on the mixing ratios of both O_3 and NO_2. Therefore, in polluted atmospheres with high levels of O_3 and NO_2, isoprene oxidation with NO_3 is especially important at night.

The major intermediates generated from isoprene oxidation with OH and NO_3 are MVK and MACR, which account for about 80% of the carbon in the initial stage of isoprene oxidation in the atmosphere (Karl et al., 2010). Accurate ambient measurement of MVK and MACR is a first-order requirement for testing concepts of the reaction pathways of isoprene (Liu et al., 2016). In addition, measurement of isoprene and its oxidation products provides useful information about the magnitude and location of isoprene sources (Karl et al., 2009;Guo et al., 2012;Su et al., 2016). Furthermore, diurnal cycles and compound correlations of isoprene and its oxidation products MVK and MACR at a particular site can yield information about the locally dominating oxidative agents, such as OH, NO_3 and O_3 (Guo et al., 2012;Millet et al., 2016), or additional sources, such as vehicular and industrial emissions (Borbon et al., 2001;Chang et al., 2014;Hsieh et al., 2016).

To deepen the scientific understanding of the biogenic–anthropogenic interactions discussed above, the aim of this study was to investigate the atmospheric oxidizing capacity by characterizing isoprene and its oxidation products (i.e. MVK and MACR) at a high-altitude mountain forest site that is highly representative of the upper atmospheric boundary layer in southern China, a region with large isoprene emissions and strong atmospheric oxidative capacity. A state-of-the-art online monitoring system was used during a field campaign in summer 2016. To our knowledge, this was the first study of isoprene observation at a remote, subtropical forested and high-altitude mountain location in southern China.

In this paper, firstly the measured concentration levels and diurnal variations of isoprene and its oxidation products are presented, then the calculated concentrations of OH and NO_3, and finally, the assessment of atmospheric reaction time of isoprene and the photochemical age of the air mass. Low isoprene levels and high (MVK+MACR)/isoprene ratios were observed and theoretical calculations confirmed that the rapidly and fully isoprene oxidation might be attributable to a strong atmospheric oxidative capacity in relation to the elevated regional complex air pollution.

2 Methods

2.1 Site description

The Pearl River Delta (PRD) region has become one of the most air-polluted areas in China, which happened along with rapid economic growth and urbanization over the past few decades (Chan and Yao, 2008). It was reported that the OH levels in the PRD were extremely high, with daily peak values of $1.5–2.6\times10^7$ molecules cm^{-3} and nocturnal concentrations within the range of $0.5–3\times10^6$ molecules cm^{-3} (Hofzumahaus et al., 2009;Lu et al., 2012;Lu et al., 2014), significantly higher than the global mean OH level ($\sim1.1\times10^6$ molecules cm^{-3}) (Naik et al., 2013;Lelieveld et al., 2016). The high atmospheric oxidative capacity has the potential to influence the local and regional air chemistry around the PRD.

To the north of the PRD region lies the Nanling Mountains, an important geographic boundary in southern China separating the temperate areas in the north from subtropical regions in the southeast coast (Siu et al., 2005). The mountain range straddles over 1,400 km from west to east across the borders of four provinces (i.e. Guangxi, Hunan, Guangdong and Jiangxi). The area is the key pathway for the long-range transport of air pollutants from the PRD region to middle-eastern China, particularly during summer, when the southwesterly winds prevail. With a forestry area of 53,600 km^2, the Nanling mountain range holds the best preserved and the most representative subtropical evergreen broad-leaved forest in the regions of the same latitude in the world. The trees and shrubs in this subtropical forest are mainly composed of subtropical evergreen broad-leaved trees and Moso bamboo (*Phyllostachys edulis*), both of which are well known to be strong isoprene emitters (Bai et al., 2016a;Bai et al., 2017). Therefore, the Nanling Mountains is an ideal location for studying anthropogenic–biogenic interactions for its high natural emissions and its proximity to anthropogenic pollution sources. So far, however, no isoprene measurements have been conducted in this important area.

The sampling site (24° 41′ 56″ N, 112° 53′ 56″ E, 1,690 m a.s.l.) is located at the summit of Mt. Tian Jing in the centre of Guangdong Nanling National Nature Reserve (24° 37′–24° 57′ N, 112° 30′–113° 04′ E, with an area of 58,368 hm^2), southern part of the Nanling Mountains (Fig. 1). Mt. Tian Jing is the highest mountain within a radius of 24 km, with no obstacles around. The site is relatively far from urban and industrial areas, and free of any emissions from local anthropogenic activities; thus serving as one of the national air quality background monitoring stations in China. To the south are the city clusters of the PRD region (200 km north of the metropolitan Guangzhou), which is one of the most urbanized areas in China. During the southwest monsoon (June to September), polluted air from the PRD region or even Southeast Asian may reach the sampling site (Siu et al., 2005;Lin et al., 2017). As the Nanling site is a high altitude mountaintop site in a remote region, and highly representative of the upper atmospheric boundary layer in southern China, measurements of surface isoprene and other species can well represent a large-scale situation.

2.2 Measurement Techniques

2.2.1 Sampling and analysis of VOCs

The continuous sampling and analysis of ambient VOCs at the Nanling site were conducted automatically by a state-of-the-art online cryogen-free GC–MS system in summer 2016 (*i.e.*, July 15–August 17). The time resolution was 1 h. The VOC measurement instruments were placed inside a two-story building. The sampling tube inlet was located 1.5 m above the rooftop of the building. Ambient air samples were drawn through a 5 m perfluoroalkoxy tube (OD 1/4 inch). The system consisted of a cryogen-free trap pre-concentration device (TH-PKU 300B, Wuhan Tianhong Instrument Co. Ltd., China) and an Agilent 7890A GC/ 5977E MS system (Agilent Tec. USA). The details of this system are described elsewhere (Wang et al., 2014;Li et al., 2016). Briefly, the ambient air was sampled and pumped into an electronic refrigeration and pre-concentration system for 5 min every hour. In order to prevent particulate matter from entering into the sampling system, a Teflon filter was placed in front of the sample inlet. CO_2 and moisture were removed by a soda asbestos tube and a waterremoval trap, respectively, before VOC analysis. VOCs were separated on a semipolar column (DB-624, 60 m × 0.25 mm ID × 1.4 µm, J&W Scientific, USA) and then quantified using a quadrupole MS detector with a full-scan mode.

Rigorous QA (quality assurance) and QC (quality control) procedures were performed through the entire measurement period. To assess the wall loss of VOCs when passing through the sampling tube, canister sampling at the sampling tube inlet was conducted simultaneously with the online measurements, and samples were analysed using the offline mode of the instrument at night of the same day. Twenty-four off-line samples were collected by canisters during the campaign. The slope and correlation coefficient (R^2) of a plot between off-line samples and online measurements for isoprene, MVK and MACR are 0.98–1.01 and >0.99, respectively. Calibration curves were established for each individual species at seven different concentrations ranging from 10 to 2,000 pptv before sample analysis. The GC–MS system was also calibrated using four internal standards (Bromochloromethane, 1,4-Difluorobenzene, Chlorobenzene-d5 and 4-Bromofluorobenzene). A mixture of 55 non-methane hydrocarbons (NMHCs) and a mixture of oxygenated VOCs (OVOCs) (Linde Electronics and Specialty Gases, USA) were used to make the certificated curves for calibration. R^2 values of calibration curves were >0.99 for all species. Daily calibrations were performed with ±10% variations with reference to the calibration curve results. The method detection limit (MDL) for isoprene, MVK and MACR quantified with this system was 4, 15 and 10 pptv, respectively.

2.2.2 Continuous measurements of trace gases and meteorological parameters

Ozone (O_3) was measured using a commercial UV photometric instrument (model 49i, Thermo Scientific, Inc.), which has a detection limit of 0.5 ppbv. Oxides of nitrogen (NO-NO_2-NO_x) were measured at 1 min resolution using chemiluminescence analyser (Thermo Scientific 42i-TL), which has a detection limit of 0.05 ppbv. Sulfur dioxide (SO_2) was measured by pulsed UV fluorescence (model 43i-TLE, Thermo Scientific, Inc.) with a detection limit of 0.05 ppbv. Carbon monoxide (CO) was monitored using a gas filter correlation infrared absorption trace level analyser (model 48i-TLE, Thermo Scientific, Inc.). A NIST-traceable standard was applied daily to calibrate the analysers by using Thermo 146i multi-gas calibrator. The zero and span drift calibrations of the analysers were conducted every two days.

In addition to the above chemical measurements, key meteorological parameters were monitored by an integrated sensor suite (WXT520, Vaisala, Inc., Finland) including temperature, relative humidity, wind speed, wind direction and precipitation.

2.3 OH and NO_3 concentrations estimated using photochemical box model

Since the OH and NO_3 concentrations were not measured in this campaign, they were estimated by using a photochemical box model incorporating Master Chemical Mechanism (PBM-MCM). Since MCM (v3.2) adopts a near-explicit mechanism, involving 5,900 chemical species and around 16,500 reactions, it has a good performance on calculating free radicals and intermediate products (Jenkin et al., 1997; Jenkin et al., 2003; Saunders et al., 2003). It is noteworthy that the PBM-MCM model only considers dry deposition, whereas vertical and horizontal transport is not considered in terms of atmospheric physical processes. In this study, the observed hourly data of air pollutants (O_3, NO, NO_2, CO, SO_2 and VOCs) and meteorological parameters (temperature and relative humidity) for the sampling period were input into the model for simulations. The model output included the averaged concentrations of OH and NO_3 radicals. More detailed descriptions of the PBM-MCM are provided in Ling et al. (2014), Guo et al. (2013) and Cheng et al. (2010).

2.4 Calculation of the atmospheric reaction time of isoprene

To calculate the atmospheric reaction time of isoprene, a "sequential reaction approach" based on isoprene's oxidation mechanism and empirical relationship between isoprene and its oxidation products was used in this study (Stroud et al., 2001;de Gouw, 2005;Roberts et al., 2006). It is noteworthy that this simplified calculation approach assumes that no fresh emissions of isoprene are introduced and isoprene emissions are constant during the process. The expression is purely chemical and does not account for the effects of mixing and transport. We also implicitly assume that the processing time of the air mass was identical for MVK and MACR and there were no additional sources of MACR and MVK apart from the oxidation of isoprene. More description about the calculation is given in the Text S1.

2.5 Photochemical age of the air mass

Measurements of certain anthropogenic VOCs (e.g. aromatic VOCs) provided us a chance to evaluate the aging degree of the air mass. Photochemical age is usually used to represent the aging degree of the air mass, and it can be calculated by the ratios of two VOC species that share common emission sources but with large different reactivities with OH (de Gouw, 2005;Shiu et al., 2007;Parrish et al., 2007;Yuan et al., 2012;Yang et al., 2017). Although mixing of fresh emissions with aged air masses will introduce substantial uncertainties in the determination of photochemical age, it still provides useful measures of photochemical processing in the atmosphere. In this study, we chose three pairs of aromatic species: toluene/benzene, ethylbenzene/benzene, and m,p-xylene/benzene. Details about the photochemical age calculation are given in the Text S2.

In addition, the open source R package "openair" (Carslaw, 2015;Carslaw and Ropkins, 2012) was utilized for data analysis and graph plotting (see Text S3).

3 Results and Discussion

3.1 Time series of meteorology and trace gases

The time series of selected meteorological parameters and trace gases are presented in 1 hour averages (Fig. 2). Discontinuities in the figure indicate that either no data were available due to the calibration and maintenance of the instruments or the values were below the MDL for those time periods. During the study, the air masses reaching the site were mainly from the southwest and northeast directions. With the change of meteorological parameters, the mixing ratios of

Atmos. Chem. Phys. Discuss., https://doi.org/10.5194/acp-2018-336
Manuscript under review for journal Atmos. Chem. Phys.
Discussion started: 16 May 2018

air pollutants changed correspondingly. In particular, from July 23 to 27, concentrations of anthropogenic pollutants (SO_2, CO and aromatic VOCs) dramatically increased, and were probably affected by regional transport. During July 28–31, due to the relatively higher temperature and lower surface wind, the emissions of isoprene were enhanced, and the dispersion of isoprene and its oxidation products was reduced, resulting in elevated levels of these species in the air. In addition, there was a notable decrease in concentrations of both isoprene and its oxidation products in August 2–3 caused by continuous rain during the typhoon NIDA.

The average hourly levels of isoprene, MVK, MACR, benzene, toluene, ethylbenzene and m,p-xylene were 287 $\pm$ 32 pptv (4–2605 pptv), 293 $\pm$ 22 pptv (16–1244 pptv), 73 $\pm$ 6 pptv (10–442 pptv), 51 $\pm$ 8 pptv (4–992 pptv), 154 $\pm$ 20 pptv (19–1770 pptv), 47 $\pm$ 6 pptv (2–499 pptv) and 38 $\pm$ 4 pptv (7–274 pptv), respectively. The concentrations of O_3, NO_2, NO, CO and SO_2 ranged from 14.4 to 130.6 ppbv (mean = 53.5), 0.9 to 10.5 ppbv (mean = 2.4), 0.6 to 8.7 ppbv (mean = 0.7), 40.8 to 684.4 ppbv (mean = 260.3) and 0.5 to 3.1 ppbv (mean = 0.9), respectively. The average temperature was 19.2 $\pm$ 0.1 ℃ and the relative humidity was 92.1 $\pm$ 0.6 %.

Isoprene concentrations vary in locations and seasons due to the difference in forest types, ambient oxidation processes and related meteorological parameters (e.g. temperature and sunlight). Surprisingly, comparison revealed that the isoprene level in this study was much lower than that observed at other sites of the same type of forest, either in China or around the world (Table 1), particularly if considering a fact that potentially strong isoprene emitters, like evergreen broad-leaved trees and shrubs, are widely seen in this low latitude subtropical-forested region (Bai et al., 2016a;Bai et al., 2017). Although the high-altitude feature (1,690 m a.s.l.) of this mountain site may lower the observed isoprene levels as compared with the forest canopy underneath the site, it is interesting to find that the daytime isoprene concentration (377 $\pm$ 46 pptv) in the hottest months (July–August) of the year was 0.5–1.0 times lower than the values observed at the same latitude subtropical-forested sites in Southern China (e.g. yearly value of 760 pptv at DingHu Mountain, and summer average of 554 pptv in HongKong) (Chen et al., 2010;Wu et al., 2016), and even slightly lower than the autumn values (410 pptv) of a site (3,250 m a.s.l.) located on the Tibetan Plateau (Bai et al., 2016b). Furthermore, O_3 and NO_x levels at this site were generally higher than the observations available in other forest studies worldwide (Table 1), likely suggesting the relevance of the low observed isoprene levels with the complex atmospheric pollution in this region.

3.2 Diurnal variations

The diurnal behaviours of isoprene, MVK and MACR are influenced by a number of chemical (e.g. oxidants levels) and meteorological (e.g. temperature) factors. Fig. 3 shows the average diurnal patterns of isoprene, MVK and MACR. The diurnal variations of (MVK+MACR)/isoprene ratios, temperature, O_3, NO_2, NO and CO are also shown in the figure. During the sampling periods (July 15–August 17, 2016), the sunrise and sunset times were 05:49–06:03 and 18:57–19:15 LT, respectively. The mixing ratio of isoprene started increasing at 7 a.m., peaked at 2 p.m., and then gradually decreased to a low level at night, and remained at this level until 7 a.m. of the next day. The levels of isoprene, MVK and MACR decreased substantially at 6 a.m., likely due to the expansion of the atmospheric boundary layer (ABL) and entrainment of oxidants-rich free tropospheric (FT) air into the ABL (Vilà-Guerau de Arellano et al., 2011). The hourly averaged daytime (06:00–18:00 LT) levels of isoprene (377 ± 46 pptv, $p < 0.01$) and MVK (332 ± 32 pptv, $p < 0.01$) were both higher than their average nighttime values (159 ± 35 pptv and 252 ± 28 pptv, respectively). However, the daytime level of MACR (66 ± 7 pptv) was slightly lower than its average nighttime value (81 ± 10 pptv).

Isoprene mixing ratios were consistently higher during daytime and lower at nighttime, indicating higher net production of isoprene during the day compared to the night. Daytime MVK and MACR are formed dominantly from the reaction of isoprene with OH radical (Reissell and Arey, 2001). The rapid decrease in isoprene after sunset was attributed to the reaction with NO_3 radical (Apel, 2002). In this study, the MVK mixing ratios during the day were higher than those during the night, suggesting that the MVK was mainly formed from the reaction of daytime produced isoprene with OH. In addition, the remaining isoprene after daytime photochemical loss reacted with NO_3 at night, contributing to the nighttime MVK formation. Although the yield of MACR and MVK from isoprene NO_3-oxidation are the same (0.035) and MACR react faster with NO_3 than MVK (Table S1). Surprisingly, the nighttime MACR levels were slightly higher than those during the day, probably due to the reaction of daytime residual isoprene with high levels of nighttime O_3, as the yield of MACR from isoprene O_3-oxidation is nearly 2 times higher than that of MVK (Table S1). In this study, due to the remote and high-altitude nature of the site, both daytime isoprene photochemistry and nighttime NO_3 chemistry played an important role in the diurnal patterns of isoprene, MVK and MACR. Interestingly, higher MACR levels at night than that during the day may attributed to the high nighttime O_3.

In this remote forest area, isoprene oxidation was the dominating source of MVK and MACR. During the daytime and nighttime periods, the (MVK+MACR)/isoprene ratio at a particular location is driven in part by the dominant daytime OH and nighttime NO_3 chemistry, which consumes isoprene while producing and destroying MVK and MACR. The ratio is expected to depend on factors such as the isoprene emission rate, the NO_x-dependent radical concentration, the degree of atmospheric mixing, and distance from isoprene emitters (Montzka et al., 1995;Biesenthal et al., 1998). In this study, it is somewhat surprising that despite these effects, the calculated ratio is quite high, averaging 4.0 ± 0.8, as shown in Fig. 3. The ratio at nighttime hours (6.3 ± 1.4, $p<0.01$) is much higher than that (1.9 ± 0.5) during daytime hours. The diurnal pattern of the ratio of this study is consistent with the results by Biesenthal et al. (1998) and Apel (2002), with both studies showing higher values during nighttime hours. The average ratio of (MVK + MACR)/isoprene is notably higher than that (0.12 and 2.0 for daytime and nighttime hours, respectively) by Apel (2002), in which sampling site was ~12 m above a rural forest canopy. The high (MVK + MACR)/isoprene ratios in this study are in close agreement with Kuhn et al. (2007), who reported an increase of the ratios with the height within the ABL. In addition, studies have shown that enhanced levels of the (MVK+MACR)/isoprene ratio are expected in environments where the air mass has aged under high-NO_x and high-oxidants conditions (Apel, 2002). In this study, the site was in a relatively high NO_x and oxidants regime and this may have contributed to the observed high ratios. This remarkably high (MVK+MACR)/isoprene ratio were indicative of a remarkably high oxidation capacity, likely suggesting that isoprene was fully oxidized at this site in both daytime and nighttime periods.

3.3 Estimated concentrations of OH and NO_3 radical

It is well known that OH radical is largely responsible for the daytime isoprene removal while NO_3 radical become more important in the oxidation of isoprene, MVK and MACR at night (Starn et al., 1998;Reissell and Arey, 2001). The diurnal profiles of model-calculated OH and NO_3 radical are shown in Fig. 4.

3.3.1 Daytime OH

The average hourly daytime OH concentration estimated by PBM-MCM at this remote forest site was $7.3 \pm 0.5 \times 10^6$ molecules cm^{-3} (0.36 ± 0.03 pptv), with a median value of 7.7×10^6 molecules cm^{-3}. Peaks in concentrations ($14.4 \pm 0.8 \times 10^6$ molecules cm^{-3}) appeared at 12:00 LT when the solar radiation was usually the strongest, and then gradually the concentrations decreased to the lowest levels before sunset. The calculated average OH level in this study is consistent with the results in the PRD region (~8×10^6 molecules cm^{-3}) (Xiao et al., 2009;Yang et al., 2017;Hofzumahaus et al., 2009). And the range of estimated mixing ratios of daytime OH (3.6×10^5 to 1.9×10^7 molecules cm^{-3}) in this work generally agrees with the daytime levels (hourly value ranged from 3.3×10^6 to 2.6×10^7 molecules cm^{-3}) observed by Xiao et al. (2009), Hofzumahaus et al. (2009) and Lu et al. (2012) at rural site in the PRD region. The modelled daytime peak OH value is much higher than those observed daytime maxima at remote forest areas such as Blodgett forest in California (4×10^6 molecules cm^{-3}) (Mao et al., 2012), boreal forest in Finland (3.5×10^6 molecules cm^{-3}) (Hens et al., 2014), pine forest in Alabama (1×10^6 molecules cm^{-3}) (Feiner et al., 2016) and Mount Tai in Central China (5.7×10^6 molecules cm^{-3}) (Kanaya et al., 2009). Limited studies performed in the PRD region have confirmed the strong atmospheric oxidizing capacity in the polluted atmosphere of this region (Hofzumahaus et al., 2009;Lu et al., 2012;Xue et al., 2016;Ma et al., 2017;Li et al., 2018). The high model-derived concentrations of OH in this study indicate that the atmospheric oxidative capacity of this forested region was strong, which facilitates fast oxidation of daytime isoprene.

3.3.2 Nocturnal NO_3

The estimated average nighttime hourly NO_3 level was $6.0 \pm 0.5 \times 10^8$ molecules cm^{-3} (29 ± 3 pptv). The estimated levels of nighttime NO_3 for this remote mountain site are comparable to the results (~40 pptv) obtained at a semi-rural mountain site (825 m a.s.l.) (Sobanski et al., 2016) and lower than the levels (~70 pptv) observed at a high-altitude (2,280 m a.s.l.) mountain site (Chen et al., 2011). The NO_3 levels in this study were higher than that (11 pptv) modelled by Guo et al. (2012) and close to that (~31 pptv) observed by Brown et al. (2016) both at a mountaintop site (640 m a.s.l.) in Hong Kong. The mixing ratios of NO_3 started steady increasing at 7 p.m., peaked at 8 p.m., then rose gradually after midnight, and peaked again at 2 a.m. of the next day. The nocturnal variation of NO_3 is similar to that of O_3 (peak at 8 p.m.). At our study site, the average nighttime mixing ratios of NO_2 (2.5 ± 0.1 ppbv) and O_3 (55.5 ± 2.1 ppbv) were relatively high when compared with other remote forest sites (NO_2 < 1 ppbv, O_3 < 30 ppbv), providing more favourable conditions for the NO_3 formation. In addition, in the surface layer of urban areas, NO_3 is generally low due to the existence of continuously anthropogenic NO as an important NO_3 sink; however, in remote or high-altitude mountain regions with cleaner air aloft (e.g. in the upper ABL or FT), higher NO_3 are often observed (Chen et al., 2011;Sobanski et al., 2016;Wang et al., 2017). The vertical profiles of NO_3 (Fish et al., 1999;Friedeburg et al., 2002;Stutz et al., 2004) suggest that the NO_3 concentration increases with altitude, with a significant fraction existing in the upper ABL or FT (Allan et al., 2002). This is consistent with our results obtained at this high-elevation mountain site. Therefore, the relatively high nighttime NO_3 concentrations at this high-altitude mountain site may lead to fast decay of daytime residual isoprene and consequently contribute to MVK and MACR formation.

3.4 Atmospheric reaction time of isoprene

As MVK and MACR are dominant first-generation reaction products from isoprene oxidation, a relationship can be expected between the concentrations of isoprene and these species (Biesenthal et al., 1997). The ratios of MVK/isoprene and MACR/isoprene provide useful information on the oxidation process of isoprene in an air mass (Stroud et al., 2001;Apel, 2002;Roberts et al., 2006;Kuhn et al., 2007;Xie et al., 2008;Liu et al., 2009;Guo et al., 2012;Wolfe et al., 2016). In this study, since the OH and NO_3 concentrations were not measured and varies as an air mass ages, we prefer to use the term "exposure" (Jimenez et al., 2009;Wolfe et al., 2016;de Gouw, 2005), defined here as the product of radical concentration and reaction time for the isoprene in the atmosphere between emission and detection.

Fig. 5 compares the observed relationship of observed MVK/isoprene and MACR/isoprene ratios against theoretical trends predicted by the sequential reaction model for the daytime and nighttime hours. It can be seen that the observed ratios of MVK/isoprene versus MACR/isoprene exhibit a tight linear correlation (R^2=0.68 and 0.72 for daytime and nighttime periods, respectively). The measured data fit the predicted line well, although most of the measured data are above the predicted line, consistent with the observations of several previous studies (Stroud et al., 2001;Apel, 2002;Guo et al., 2012). This might be caused by a continuous supply of MVK and MACR from surrounding forest trees during the daytime hours and additional source from oxidation by daytime NO_3 and nighttime OH (Brown et al., 2005;Faloona et al., 2001), which were not taken into account in the sequential reaction modeling. The theoretical slope agrees well with observations, indicating exposures of 0.1–12 $\times 10^6$ OH cm^{-3} h and 4–28 $\times 10^8$ NO_3 cm^{-3} h for daytime and nighttime periods, respectively. For a typical daytime average OH concentration of 8 $\times 10^6$ molecules cm^{-3} (Xiao et al., 2009;Yang et al., 2017;Hofzumahaus et al., 2009) and nighttime average NO_3 concentration of 5 $\times 10^8$ molecules cm^{-3} (Guo et al., 2012;Brown et al., 2016), this corresponds to daytime and nighttime processing times of 0.01–1.5 h and 0.8–5.6 h, respectively.

Exposures can be calculated from observed daughter/parent ratios. Fig. 6a shows the derived exposures from MVK/isoprene and MACR/isoprene ratios. Calculated daytime OH exposures and nighttime NO_3 exposures range from 1.0 $\times 10^5$ to 1.3 $\times 10^7$ molecules cm^{-3} h and 3.5$\times 10^8$ to 3.2 $\times 10^9$ molecules cm^{-3} h, respectively. OH and NO_3 exposures derived from two methods exhibit a good linear correlation (R^2=0.63 and 0.70 for OH and NO_3, respectively), and results derived from MACR are 4% and 18% lower than those from MVK on average, respectively, and we use the mean of these two values. The median and mean OH exposure is 1.9 and 2.5 × 10^6 molecules cm^{-3} h, respectively. For NO_3 exposure, the median and mean value is close (15.8 and 16.2 × 10^8 molecules cm^{-3} h, respectively). The mean daytime and nighttime isoprene reaction time are 0.3 and 3.2 hours, respectively, assuming daytime OH = 8.0 × 10^6 molecules cm^{-3} and nighttime NO_3 = 5 × 10^8 molecules cm^{-3}. The isoprene processing time is mainly relevant to OH and NO_3 mixing ratios, which varied spatially and temporarily, and the proximity to isoprene sources.

To obtain the detailed profiles of the isoprene atmospheric reaction time at the site, we calculated them which based on the modelled OH and NO_3 results in this study. Fig. 6b shows the derived reaction times from MVK/isoprene and MACR/isoprene ratios. Reaction times derived from two methods exhibit a significant linear correlation (R^2=0.91 and 0.90 for daytime and nighttime, respectively), and results derived from MACR are 13% lower than those from MVK on average, and we use the mean of these two values. The calculated isoprene reaction time during the day is between 0.01 and 14.43 hours, with median and mean values of 0.27 and 1.39 hours, respectively. The isoprene reaction time during the night was calculated to be between 0.30 and 16.44 hours, with median and average values of 4.10 and 4.49 hours. The longer isoprene reaction time at night than during the day is probably due to the lower reaction rate of isoprene with NO_3 than with OH. The daytime residual MVK and MACR after sunset may also have significant impacts on the calculated nighttime reaction time, as the life time of MVK and MACR for reaction with NO_3 is long (0.5 years and 72 hours at a 12-h nighttime average NO_3 of 5.0 × 10^8 molecules cm^{-3}, respectively). The median daytime reaction time (0.27 hours) of measured isoprene was slightly lower than the theoretical lifetime of isoprene (0.4 hours at 12-h daytime averaged [OH] = 8.0 × 10^6 molecules cm^{-3}). In this study, the average distance between the sampling site and the centre of the emitting trees was about 20 km. The daytime reaction time of isoprene (16 min) in this study is lower than that (~30 min) of Guo et al. (2012) in which the sampling site was 5 km away from the centre of the large forests in Hong Kong. And that means the short reaction time of isoprene in this study was probably attributed to the high oxidants levels.

3.5 Initial mixing ratios of isoprene

To check out the magnitude of isoprene oxidation, "initial isoprene", the total isoprene emissions that have been released into the sample air masses, can be effectively calculated via reverse integration of isoprene's first-order oxidation (Wolfe et al., 2016):

$$[ISOP]_0 = [ISOP] \times e^{(k \times EXPO)}, \quad (1)$$

Where $[ISOP]_0$ is the initial isoprene, representing the amount of isoprene that an air parcel would have to start with to generate the amount of isoprene, MVK and MACR observed. $[ISOP]$ is the observed isoprene. k is the reaction rate coefficients for the reactions of isoprene with OH and NO_3 radical. $EXPO$ is the calculated OH and NO_3 exposures.

Fig. 7a shows plots of the initial isoprene versus the observed isoprene. The daytime initial isoprene mixing ratios (1213 ± 108 pptv) is much higher than the observed values (377 ± 46 pptv). It is noteworthy that the nighttime initial isoprene by this approach may be overestimated due to the daytime residual MVK and MACR into the night. The daytime initial mixing ratios of isoprene are 1–20 times higher than the observed levels, with median and mean values of 2.1 and 4.3, respectively.

Scatter plots of calculated initial isoprene versus measured MVK+MACR during daytime hours are also given in Fig. 7b, and a good correlation (R^2=0.71) was obtained. Since the slope is related to the yield of (MVK+MACR) from OH-initiated reaction of isoprene and further oxidation of those two products with OH, data points away from the dashed line are likely due to chemical loss of MVK and MACR and/or the influence of continuous emissions of isoprene. These results further confirmed that isoprene was fully oxidized in the air masses.

3.6 Aging degree of the air mass

Fig. 8 shows the calculated photochemical age (PA) from daytime toluene/benzene (referred to as T/B), ethylbenzene/benzene (E/B), and m,p-xylene/benzene (X/B) ratios. PA derived from the three methods exhibit a good linear correlation (R^2=0.82 and 0.79 for $PA_{T/B}$ versus $PA_{X/B}$ and $PA_{E/B}$ versus $PA_{X/B}$, respectively). Results derived from X/B are 37% and 24% lower than those from T/B and E/B on average, respectively, and we use the mean of these three values in this study. The higher mean values than median values for all methods indicating certain impacts of outflow from urban areas (e.g. the PRD region) (Suthawaree et al., 2012), when the polluted air mass arriving from those areas transported to the site leads to higher photochemical age (1.4–8.2 days). The median and mean PA are 3.8 and 12.4 h, respectively. The average PA in this study was about twice times of the observations (6–7 hours) in a suburban site in the PRD region (Yang et al., 2017), indicating a more aged atmospheric environment in this remote site.

4 Conclusions

In this study, isoprene and its major intermediate oxidation products MVK and MACR were simultaneously observed in real-time in 2016 summer season at a high-altitude mountain forest site located at the Nanling Mountains in southern China. Although the sampling site was surrounded with subtropical evergreen broad-leaved trees which are strong isoprene emitters, the observed isoprene level (377 ± 46 pptv) was found to be significantly lower than other remote forest studies, while (MVK+MACR)/isoprene ratio (4.0 ± 0.8) was relatively higher. Based on the observations, we hypothesized that the lower isoprene levels in the study forest might be attributable to a strong atmospheric oxidative capacity in relation to the elevated regional complex air pollution.

To validate this hypothesis, high daytime OH and nighttime NO_3 radical concentrations were estimated by using a PBM-MCM, with average hourly mixing ratios of $7.3 \pm 0.5 \times 10^6$ (0.36 ± 0.03 pptv) and $6.0 \pm 0.5 \times 10^8$ (29 ± 3 pptv) molecules cm^{-3}, respectively. The modelled values are comparable to those observations conducted in the adjacent PRD region. The high model-derived radical levels indicate the strong atmospheric oxidative capacity in this subtropical-forested region, which facilitates fast isoprene oxidation and subsequently contributes to the MVK and MACR formation.

In addition, the term "exposure" was used to express the isoprene processing, with mean daytime OH and nighttime NO_3 exposure of 2.5×10^6 and 16.2×10^8 molecules cm^{-3} h was obtained, respectively. Short atmospheric reaction times of isoprene during the day (0.27 h) and night (4.10 h) were subsequently calculated based on the estimated radical concentrations. Also, the initial isoprene was 4.3 times higher than the observed isoprene, and the photochemical age (12.4 h) at this site was about twice times of that in the PRD region. These indicate that the isoprene was rapidly and fully oxidized at this aged atmospheric environment.

To the best of our knowledge, there are no direct measurements of isoprene and its first-stage oxidation products at this remote, subtropical forested and high-altitude mountain location in southern China; thus, the results presented here constitute the first measurement-constrained evaluation of the early-stage isoprene oxidation. In this regard, the current work has highlighted that the air quality and ecological environment of this forest was affected by the highly polluted air in the PRD region and has led to enhanced oxidation capacity of the forest′s atmosphere. Continued field observations and further studies are crucial for understanding the relatively high oxidative capacity of this region and for exploring the feedback of forest ecosystems to the increasing atmospheric oxidizing conditions.

Acknowledgments

This work was supported by the National Natural Science Foundation of China (91544215, 41373116). The authors thank Jie Ou, the chief engineer of Shaoguan Environmental Monitoring Central Station, for the help during the sampling campaign. We also acknowledge Dr. David Carslaw for the provision of the R package “openair” (http://www.openair-project.org) used in this publication. We also thank the Team BlackTree for providing an aerial photo of the Nanling site in Fig. 1c.

References

Acton, W. J. F., Schallhart, S., Langford, B., Valach, A., Rantala, P., Fares, S., Carriero, G., Tillmann, R., Tomlinson, S. J., Dragosits, U., Gianelle, D., Hewitt, C. N., and Nemitz, E.: Canopy-scale flux measurements and bottom-up emission estimates of volatile organic compounds from a mixed oak and hornbeam forest in northern Italy, Atmos Chem Phys, 16, 7149-7170, 10.5194/acp-16-7149-2016, 2016.

Allan, B. J., Plane, J. M. C., Coe, H., and Shillito, J.: Observations of NO_3 concentration profiles in the troposphere, Journal of Geophysical Research: Atmospheres, 107, ACH 11-11-ACH 11-14, 10.1029/2002jd002112, 2002.

Alves, E. G., Jardine, K., Tota, J., Jardine, A., Yanez-Serrano, A. M., Karl, T., Tavares, J., Nelson, B., Gu, D. S., Stavrakou, T., Martin, S., Artaxo, P., Manzi, A., and Guenther, A.: Seasonality of isoprenoid emissions from a primary rainforest in central Amazonia, Atmos Chem Phys, 16, 3903-3925, 10.5194/acp-16-3903-2016, 2016.

Apel, E. C.: Measurement and interpretation of isoprene fluxes and isoprene, methacrolein, and methyl vinyl ketone mixing ratios at the PROPHET site during the 1998 Intensive, Journal of Geophysical Research, 107, 15, 10.1029/2000jd000225, 2002.

Bai, J., Guenther, A., Turnipseed, A., Duhl, T., and Greenberg, J.: Seasonal and interannual variations in whole-ecosystem BVOC emissions from a subtropical plantation in China, Atmos Environ, 161, 176-190, 10.1016/j.atmosenv.2017.05.002, 2017.

Bai, J. H., Guenther, A., Turnipseed, A., Duhl, T., Yu, S. Q., and Wang, B.: Seasonal variations in whole-ecosystem BVOC emissions from a subtropical bamboo plantation in China, Atmos Environ, 124, 12-21, 10.1016/j.atmosenv.2015.11.008, 2016a.

Bai, Y., Bai, Z., and Li, W.: Characteristics and sources analysis of atmospheric volatile organic compounds in the Tibetan Plateau, Acta Scientiae Circumstantiae, 36, 2180-2186, 10.13671/j.hjkxxb.2016.0008, 2016b.

Biesenthal, T., Wu, Q., Shepson, P. B., Wiebe, H. A., Anlauf, K. G., and Mackay, G. I.: A study of relationships between isoprene, its oxidation products, and ozone, in the Lower Fraser Valley, BC, Atmos Environ, 31, 2049-2058, 1997.

Biesenthal, T. A., Bottenheim, J. W., Shepson, P. B., and Brickell, P. C.: The chemistry of biogenic hydrocarbons at a rural site in eastern Canada, Journal of Geophysical Research-Atmospheres, 103, 25487-25498, 10.1029/98jd01848, 1998.

Borbon, A., Fontaine, H., Veillerot, M., Locoge, N., Galloo, J. C., and Guillermo, R.: An investigation into the traffic-related fraction of isoprene at an urban location, Atmos Environ, 35, 3749-3760, 10.1016/S1352-2310(01)00170-4, 2001.

Brown, S. S., Osthoff, H. D., Stark, H., Dube, W. P., Ryerson, T. B., Warneke, C., de Gouw, J. A., Wollny, A. G., Parrish, D. D., Fehsenfeld, F. C., and Ravishankara, A. R.: Aircraft observations of daytime NO_3 and N_2O_5 and their implications for tropospheric chemistry, Journal of Photochemistry and Photobiology a-Chemistry, 176, 270-278, 10.1016/j.jphotochem.2005.10.004, 2005.

Brown, S. S., Dube, W. P., Tham, Y. J., Zha, Q. Z., Xue, L. K., Poon, S., Wang, Z., Blake, D. R., Tsui, W., Parrish, D. D., and Wang, T.: Nighttime chemistry at a high altitude site above Hong Kong, Journal of Geophysical Research-Atmospheres, 121, 2457-2475, 10.1002/2015jd024566, 2016.

Carslaw, D. C., and Ropkins, K.: openair - An R package for air quality data analysis, Environmental Modelling & Software, 27-28, 52-61, 10.1016/j.envsoft.2011.09.008, 2012.

Chan, C. K., and Yao, X.: Air pollution in mega cities in China, Atmos Environ, 42, 1-42, 10.1016/j.atmosenv.2007.09.003, 2008.

Chang, C.-C., Wang, J.-L., Candice Lung, S.-C., Chang, C.-Y., Lee, P.-J., Chew, C., Liao, W.-C., Chen, W.-N., and Ou-Yang, C.-F.: Seasonal characteristics of biogenic and anthropogenic isoprene in tropical–subtropical urban environments, Atmos Environ, 99, 298-308, 10.1016/j.atmosenv.2014.09.019, 2014.

Chen, C. M., Cageao, R. P., Lawrence, L., Stutz, J., Salawitch, R. J., Jourdain, L., Li, Q., and Sander, S. P.: Diurnal variation of midlatitudinal NO_3 column abundance over table mountain facility, California, Atmos Chem Phys, 11, 963-978, 10.5194/acp-11-963-2011, 2011.

Chen, H. W., Ho, K. F., Lee, S. C., and Nichol, J. E.: Biogenic volatile organic compounds (BVOC) in ambient air over Hong Kong: analytical methodology and field measurement, International Journal of Environmental Analytical Chemistry, 90, 988-998, 10.1080/03067310903108360, 2010.

Claeys, M., Graham, B., Vas, G., Wang, W., Vermeylen, R., Pashynska, V., Cafmeyer, J., Guyon, P., Andreae, M. O., Artaxo, P., and Maenhaut, W.: Formation of secondary organic aerosols through photooxidation of isoprene, Science, 303, 1173-1176, 10.1126/science.1092805, 2004.

de Gouw, J. A.: Budget of organic carbon in a polluted atmosphere: Results from the New England Air Quality Study in 2002, Journal of Geophysical Research, 110, 22, 10.1029/2004jd005623, 2005.

Dreyfus, G. B., Schade, G. W., and Goldstein, A. H.: Observational constraints on the contribution of isoprene oxidation to ozone production on the western slope of the Sierra Nevada, California, Journal of Geophysical Research-Atmospheres, 107, 17, 10.1029/2001jd001490, 2002.

Edwards, P. M., Aikin, K. C., Dube, W. P., Fry, J. L., Gilman, J. B., de Gouw, J. A., Graus, M. G., Hanisco, T. F., Holloway, J., Huber, G., Kaiser, J., Keutsch, F. N., Lerner, B. M., Neuman, J. A., Parrish, D. D., Peischl, J., Pollack, I. B., Ravishankara, A. R., Roberts, J. M., Ryerson, T. B., Trainer, M., Veres, P. R., Wolfe, G. M., Warneke, C., and Brown, S. S.: Transition from high- to low-NO_x control of night-time oxidation in the southeastern US, Nat Geosci, 10, 490-+, 10.1038/Ngeo2976, 2017.

Faloona, I., Tan, D., Brune, W., Hurst, J., Barket, D., Couch, T. L., Shepson, P., Apel, E., Riemer, D., Thornberry, T., Carroll, M. A., Sillman, S., Keeler, G. J., Sagady, J., Hooper, D., and Paterson, K.: Nighttime observations of anomalously high levels of hydroxyl radicals above a deciduous forest canopy, Journal of Geophysical Research-Atmospheres, 106, 24315-24333, 10.1029/2000jd900691, 2001.

Feiner, P. A., Brune, W. H., Miller, D. O., Zhang, L., Cohen, R. C., Romer, P. S., Goldstein, A. H., Keutsch, F. N., Skog, K. M., Wennberg, P. O., Nguyen, T. B., Teng, A. P., DeGouw, J., Koss, A., Wild, R. J., Brown, S. S., Guenther, A., Edgerton, E., Baumann, K., and Fry, J. L.: Testing Atmospheric Oxidation in an Alabama Forest, J Atmos Sci, 73, 4699-4710, 10.1175/Jas-D-16-0044.1, 2016.

Fish, D. J., Shallcross, D. E., and Jones, R. L.: The vertical distribution of NO_3 in the atmospheric boundary layer, Atmos Environ, 33, 687-691, 10.1016/S1352-2310(98)00332-X, 1999.

Friedeburg, C. V., Wagner, T., Geyer, A., Kaiser, N., Vogel, B., Vogel, H., and Platt, U.: Derivation of tropospheric NO_3 profiles using off‐axis differential optical absorption spectroscopy measurements during sunrise and comparison with simulations, Journal of Geophysical Research, 107, 10.1029/2001JD000481, 2002.

Fuchs, H., Hofzumahaus, A., Rohrer, F., Bohn, B., Brauers, T., Dorn, H. P., Haseler, R., Holland, F., Kaminski, M., Li, X., Lu, K., Nehr, S., Tillmann, R., Wegener, R., and Wahner, A.: Experimental evidence for efficient hydroxyl radical regeneration in isoprene oxidation, Nat Geosci, 6, 1023-1026, 10.1038/Ngeo1964, 2013.

Gu, D., Guenther, A. B., Shilling, J. E., Yu, H., Huang, M., Zhao, C., Yang, Q., Martin, S. T., Artaxo, P., Kim, S., Seco, R., Stavrakou, T., Longo, K. M., Tota, J., de Souza, R. A. F., Vega, O., Liu, Y., Shrivastava, M., Alves, E. G., Santos, F. C., Leng, G., and Hu, Z.: Airborne observations reveal elevational gradient in tropical forest isoprene emissions, Nat Commun, 8, 15541, 10.1038/ncomms15541, 2017.

Guenther, A., Monson, R. K., and Fall, R.: Isoprene and monoterpene emission rate variability: Observations with eucalyptus and emission rate algorithm development, Journal of Geophysical Research, 96, 10799-10808, 10.1029/91JD00960, 1991.

Guenther, A., Karl, T., Harley, P., Wiedinmyer, C., Palmer, P. I., and Geron, C.: Estimates of global terrestrial isoprene emissions using MEGAN (Model of Emissions of Gases and Aerosols from Nature), Atmos Chem Phys, 6, 3181-3210, DOI 10.5194/acp-6-3181-2006, 2006.

Guenther, A. B., Jiang, X., Heald, C. L., Sakulyanontvittaya, T., Duhl, T., Emmons, L. K., and Wang, X.: The Model of Emissions of Gases and Aerosols from Nature version 2.1 (MEGAN2.1): an extended and updated framework for modeling biogenic emissions, Geoscientific Model Development, 5, 1471-1492, 10.5194/gmd-5-1471-2012, 2012.

Guo, H., Ling, Z. H., Simpson, I. J., Blake, D. R., and Wang, D. W.: Observations of isoprene, methacrolein (MAC) and methyl vinyl ketone (MVK) at a mountain site in Hong Kong, Journal of Geophysical Research-Atmospheres, 117, 13, 10.1029/2012jd017750, 2012.

Hens, K., Novelli, A., Martinez, M., Auld, J., Axinte, R., Bohn, B., Fischer, H., Keronen, P., Kubistin, D., Nolscher, A. C., Oswald, R., Paasonen, P., Petaja, T., Regelin, E., Sander, R., Sinha, V., Sipila, M., Taraborrelli, D., Ernest, C. T., Williams, J., Lelieveld, J., and Harder, H.: Observation and modelling of HO_x radicals in a boreal forest, Atmos Chem Phys, 14, 8723-8747, 10.5194/acp-14-8723-2014, 2014.

Hofzumahaus, A., Rohrer, F., Lu, K., Bohn, B., Brauers, T., Chang, C. C., Fuchs, H., Holland, F., Kita, K., Kondo, Y., Li, X., Lou, S., Shao, M., Zeng, L., Wahner, A., and Zhang, Y.: Amplified trace gas removal in the troposphere, Science, 324, 1702-1704, 10.1126/science.1164566, 2009.

Hsieh, H., Ouyang, C., and Wang, J.: Revelation of Coupling Biogenic with Anthropogenic Isoprene by Highly Time-Resolved Observations, Aerosol and Air Quality Research, 10.4209/aaqr.2016.04.0133, 2016.

Jenkin, M. E., Young, J. C., and Rickard, A. R.: The MCM v3.3.1 degradation scheme for isoprene, Atmos Chem Phys, 15, 11433-11459, 10.5194/acp-15-11433-2015, 2015.

Jimenez, J. L., Canagaratna, M. R., Donahue, N. M., Prevot, A. S., Zhang, Q., Kroll, J. H., DeCarlo, P. F., Allan, J. D., Coe, H., Ng, N. L., Aiken, A. C., Docherty, K. S., Ulbrich, I. M., Grieshop, A. P., Robinson, A. L., Duplissy, J., Smith, J. D., Wilson, K. R., Lanz, V. A., Hueglin, C., Sun, Y. L., Tian, J., Laaksonen, A., Raatikainen, T., Rautiainen, J., Vaattovaara, P., Ehn, M., Kulmala, M., Tomlinson, J. M., Collins, D. R., Cubison, M. J., Dunlea, E. J., Huffman, J. A., Onasch, T. B., Alfarra, M. R., Williams, P. I., Bower, K., Kondo, Y., Schneider, J., Drewnick, F., Borrmann, S., Weimer, S., Demerjian, K., Salcedo, D., Cottrell, L., Griffin, R., Takami, A., Miyoshi, T., Hatakeyama, S., Shimono, A., Sun, J. Y., Zhang, Y. M., Dzepina, K., Kimmel, J. R., Sueper, D., Jayne, J. T., Herndon, S. C., Trimborn, A. M., Williams, L. R., Wood, E. C., Middlebrook, A. M., Kolb, C. E., Baltensperger, U., and Worsnop, D. R.: Evolution of organic aerosols in the atmosphere, Science, 326, 1525-1529, 10.1126/science.1180353, 2009.

Jones, C. E., Hopkins, J. R., and Lewis, A. C.: In situ measurements of isoprene and monoterpenes within a south-east Asian tropical rainforest, Atmos Chem Phys, 11, 6971-6984, 10.5194/acp-11-6971-2011, 2011.

Kanaya, Y., Pochanart, P., Liu, Y., Li, J., Tanimoto, H., Kato, S., Suthawaree, J., Inomata, S., Taketani, F., Okuzawa, K., Kawamura, K., Akimoto, H., and Wang, Z. F.: Rates and regimes of photochemical ozone production over Central East China in June 2006: a box model analysis using comprehensive measurements of ozone precursors, Atmos Chem Phys, 9, 7711-7723, 10.5194/acp-9-7711-2009, 2009.

Karl, T., Guenther, A., Turnipseed, A., Tyndall, G., Artaxo, P., and Martin, S.: Rapid formation of isoprene photo-oxidation products observed in Amazonia, Atmos Chem Phys, 9, 7753-7767, 10.5194/acp-9-7753-2009, 2009.

Karl, T., Harley, P., Emmons, L., Thornton, B., Guenther, A., Basu, C., Turnipseed, A., and Jardine, K.: Efficient atmospheric cleansing of oxidized organic trace gases by vegetation, Science, 330, 816-819, 10.1126/science.1192534, 2010.

Kleinman, L., Kuang, C., Sedlacek, A., Senum, G., Springston, S., Wang, J., Zhang, Q., Jayne, J., Fast, J., Hubbe, J., Shilling, J., and Zaveri, R.: What do correlations tell us about anthropogenic–biogenic interactions and SOA formation in the Sacramento plume during CARES?, Atmos Chem Phys, 16, 1729-1746, 10.5194/acp-16-1729-2016, 2016.

Kuhn, U., Andreae, M. O., Ammann, C., Araujo, A. C., Brancaleoni, E., Ciccioli, P., Dindorf, T., Frattoni, M., Gatti, L. V., Ganzeveld, L., Kruijt, B., Lelieveld, J., Lloyd, J., Meixner, F. X., Nobre, A. D., Poschl, U., Spirig, C., Stefani, P., Thielmann, A., Valentini, R., and Kesselmeier, J.: Isoprene and monoterpene fluxes from Central Amazonian rainforest inferred from tower-based and airborne measurements, and implications on the atmospheric chemistry and the local carbon budget, Atmos Chem Phys, 7, 2855-2879, 10.5194/acp-7-2855-2007, 2007.

Lelieveld, J., Butler, T. M., Crowley, J. N., Dillon, T. J., Fischer, H., Ganzeveld, L., Harder, H., Lawrence, M. G., Martinez, M., Taraborrelli, D., and Williams, J.: Atmospheric oxidation capacity sustained by a tropical forest, Nature, 452, 737-740, 10.1038/nature06870, 2008.

Lelieveld, J., Gromov, S., Pozzer, A., and Taraborrelli, D.: Global tropospheric hydroxyl distribution, budget and reactivity, Atmos Chem Phys, 16, 12477-12493, 10.5194/acp-16-12477-2016, 2016.

Li, J., Wu, R., Li, Y., Hao, Y., Xie, S., and Zeng, L.: Effects of rigorous emission controls on reducing ambient volatile organic compounds in Beijing, China, The Science of the total environment, 557-558, 531-541, 10.1016/j.scitotenv.2016.03.140, 2016.

Li, Z., Xue, L., Yang, X., Zha, Q., Tham, Y. J., Yan, C., Louie, P. K. K., Luk, C. W. Y., Wang, T., and Wang, W.: Oxidizing capacity of the rural atmosphere in Hong Kong, Southern China, The Science of the total environment, 612, 1114-1122, 10.1016/j.scitotenv.2017.08.310, 2018.

Lin, Q., Zhang, G., Peng, L., Bi, X., Wang, X., Brechtel, F. J., Li, M., Chen, D., Peng, P., amp, apos, an, Sheng, G., and Zhou, Z.: In situ chemical measurement of individual cloud residue particles at a mountain site, South China, Atmospheric Chemistry and Physics Discussions, 2017, 1-39, 10.5194/acp-2017-23, 2017.

Link, M., Zhou, Y., Taubman, B., Sherman, J., Morrow, H., Krintz, I., Robertson, L., Cook, R., Stocks, J., West, M., and Sive, B.: A characterization of volatile organic compounds and secondary organic aerosol at a mountain site in the Southeastern United States, Journal of Atmospheric Chemistry, 72, 81-104, 10.1007/s10874-015-9305-5, 2015.

Liu, Y., Shao, M., Kuster, W. C., Goldan, P. D., Li, X., Lu, S., and de Gouw, J. A.: Source identification of reactive hydrocarbons and oxygenated VOCs in the summertime in Beijing, Environ Sci Technol, 43, 75-81, 10.1021/es801716n, 2009.

Liu, Y., Brito, J., Dorris, M. R., Rivera-Rios, J. C., Seco, R., Bates, K. H., Artaxo, P., Duvoisin, S., Jr., Keutsch, F. N., Kim, S., Goldstein, A. H., Guenther, A. B., Manzi, A. O., Souza, R. A., Springston, S. R., Watson, T. B., McKinney, K. A., and Martin, S. T.: Isoprene photochemistry over the Amazon rainforest, Proc Natl Acad Sci U S A, 113, 6125-6130, 10.1073/pnas.1524136113, 2016.

Lu, K. D., Rohrer, F., Holland, F., Fuchs, H., Bohn, B., Brauers, T., Chang, C. C., Haseler, R., Hu, M., Kita, K., Kondo, Y., Li, X., Lou, S. R., Nehr, S., Shao, M., Zeng, L. M., Wahner, A., Zhang, Y. H., and Hofzumahaus, A.: Observation and modelling of OH and HO2 concentrations in the Pearl River Delta 2006: a missing OH source in a VOC rich atmosphere, Atmos Chem Phys, 12, 1541-1569, 10.5194/acp-12-1541-2012, 2012.

Lu, K. D., Rohrer, F., Holland, F., Fuchs, H., Brauers, T., Oebel, A., Dlugi, R., Hu, M., Li, X., Lou, S. R., Shao, M., Zhu, T., Wahner, A., Zhang, Y. H., and Hofzumahaus, A.: Nighttime observation and chemistry of HO_x in the Pearl River Delta and Beijing in summer 2006, Atmos Chem Phys, 14, 4979-4999, 10.5194/acp-14-4979-2014, 2014.

Ma, Y., Lu, K., Chou, C. C. K., Li, X., and Zhang, Y.: Strong deviations from the NO-NO_2-O_3 photostationary state in the Pearl River Delta: Indications of active peroxy radical and chlorine radical chemistry, Atmos Environ, 163, 22-34, 10.1016/j.atmosenv.2017.05.012, 2017.

Mao, J., Ren, X., Zhang, L., Van Duin, D. M., Cohen, R. C., Park, J. H., Goldstein, A. H., Paulot, F., Beaver, M. R., Crounse, J. D., Wennberg, P. O., DiGangi, J. P., Henry, S. B., Keutsch, F. N., Park, C., Schade, G. W., Wolfe, G. M., Thornton, J. A., and Brune, W. H.: Insights into hydroxyl measurements and atmospheric oxidation in a California forest, Atmos Chem Phys, 12, 8009-8020, 10.5194/acp-12-8009-2012, 2012.

Millet, D. B., Baasandorj, M., Hu, L., Mitroo, D., Turner, J., and Williams, B. J.: Nighttime Chemistry and Morning Isoprene Can Drive Urban Ozone Downwind of a Major Deciduous Forest, Environ Sci Technol, 50, 4335-4342, 10.1021/acs.est.5b06367, 2016.

Montzka, S. A., Trainer, M., Angevine, W. M., and Fehsenfeld, F. C.: Measurements of 3−methyl furan, methyl vinyl ketone, and methacrolein at a rural forested site in the southeastern United States, Journal of Geophysical Research, 100, 11393-11401, 10.1029/95JD01132, 1995.

Naik, V., Voulgarakis, A., Fiore, A. M., Horowitz, L. W., Lamarque, J. F., Lin, M., Prather, M. J., Young, P. J., Bergmann, D., Cameron-Smith, P. J., Cionni, I., Collins, W. J., Dalsoren, S. B., Doherty, R., Eyring, V., Faluvegi, G., Folberth, G. A., Josse, B., Lee, Y. H., MacKenzie, I. A., Nagashima, T., van Noije, T. P. C., Plummer, D. A., Righi, M., Rumbold, S. T., Skeie, R., Shindell, D. T., Stevenson, D. S., Strode, S., Sudo, K., Szopa, S., and Zeng, G.: Preindustrial to present-day changes in tropospheric hydroxyl radical and methane lifetime from the Atmospheric Chemistry and Climate Model Intercomparison Project (ACCMIP), Atmos Chem Phys, 13, 5277-5298, 10.5194/acp-13-5277-2013, 2013.

Orlando, J. J., and Tyndall, G. S.: Laboratory studies of organic peroxy radical chemistry: an overview with emphasis on recent issues of atmospheric significance, Chem Soc Rev, 41, 6294-6317, 10.1039/c2cs35166h, 2012.

Parrish, D. D., Stohl, A., Forster, C., Atlas, E. L., Blake, D. R., Goldan, P. D., Kuster, W. C., and de Gouw, J. A.: Effects of mixing on evolution of hydrocarbon ratios in the troposphere, Journal of Geophysical Research-Atmospheres, 112, 10.1029/2006jd007583, 2007.

Reissell, A., and Arey, J.: Biogenic volatile organic compounds at Azusa and elevated sites during the 1997 Southern California Ozone Study, Journal of Geophysical Research-Atmospheres, 106, 1607-1621, Doi 10.1029/2000jd900517, 2001.

Roberts, J. M., Marchewka, M., Bertman, S. B., Goldan, P., Kuster, W., de Gouw, J., Warneke, C., Williams, E., Lerner, B., Murphy, P., Apel, E., and Fehsenfeld, F. C.: Analysis of the isoprene chemistry observed during the New England Air Quality Study (NEAQS) 2002 intensive experiment, Journal of Geophysical Research-Atmospheres, 111, 10.1029/2006jd007570, 2006.

Rohrer, F., Lu, K. D., Hofzumahaus, A., Bohn, B., Brauers, T., Chang, C. C., Fuchs, H., Haseler, R., Holland, F., Hu, M., Kita, K., Kondo, Y., Li, X., Lou, S. R., Oebel, A., Shao, M., Zeng, L. M., Zhu, T., Zhang, Y. H., and Wahner, A.: Maximum efficiency in the hydroxyl-radical-based self-cleansing of the troposphere, Nat Geosci, 7, 559-563, 10.1038/Ngeo2199, 2014.

Schulze, B. C., Wallace, H. W., Flynn, J. H., Lefer, B. L., Erickson, M. H., Jobson, B. T., Dusanter, S., Griffith, S. M., Hansen, R. F., Stevens, P. S., VanReken, T., and Griffin, R. J.: Differences in BVOC oxidation and SOA formation above and below the forest canopy, Atmos Chem Phys, 17, 1805-1828, 10.5194/acp-17-1805-2017, 2017.

Seco, R., Penuelas, J., Filella, I., Llusia, J., Molowny-Horas, R., Schallhart, S., Metzger, A., Muller, M., and Hansel, A.: Contrasting winter and summer VOC mixing ratios at a forest site in the Western Mediterranean Basin: the effect of local biogenic emissions, Atmos Chem Phys, 11, 13161-13179, 10.5194/acp-11-13161-2011, 2011.

Shiu, C. J., Liu, S. C., Chang, C. C., Chen, J. P., Chou, C. C. K., Lin, C. Y., and Young, C. Y.: Photochemical production of ozone and control strategy for Southern Taiwan, Atmos Environ, 41, 9324-9340, 10.1016/j.atmosenv.2007.09.014, 2007.

Siu, C. L., Lee, L., Li, X. D., Zhang, G., Peng, X. Z., and Zhang, L.: Biomonitoring of trace metals in the atmosphere using moss (Hypnum plumaeforme) in the Nanling Mountains and the Pearl River Delta, Southern China, Atmos Environ, 39, 397-407, 10.1016/j.atmosenv.2004.09.067, 2005.

Sobanski, N., Tang, M. J., Thieser, J., Schuster, G., Pohler, D., Fischer, H., Song, W., Sauvage, C., Williams, J., Fachinger, J., Berkes, F., Hoor, P., Platt, U., Lelieveld, J., and Crowley, J. N.: Chemical and meteorological influences on the lifetime of NO_3 at a semi-rural mountain site during PARADE, Atmos Chem Phys, 16, 4867-4883, 10.5194/acp-16-4867-2016, 2016.

Starn, T. K., Shepson, P. B., Bertman, S. B., White, J. S., Splawn, B. G., Riemer, D. D., Zika, R. G., and Olszyna, K.: Observations of isoprene chemistry and its role in ozone production at a semirural site during the 1995 Southern Oxidants Study, Journal of Geophysical Research, 103, 22425-22435, 10.1029/98JD01279, 1998.

Stroud, C. A., Roberts, J. M., Goldan, P. D., Kuster, W. C., Murphy, P. C., Williams, E. J., Hereid, D., Parrish, D., Sueper, D., Trainer, M., Fehsenfeld, F. C., Apel, E. C., Riemer, D., Wert, B., Henry, B., Fried, A., Martinez-Harder, M., Harder, H., Brune, W. H., Li, G., Xie, H., and Young, V. L.: Isoprene and its oxidation products, methacrolein and methylvinyl ketone, at an urban forested site during the 1999 Southern Oxidants Study, Journal of Geophysical Research-Atmospheres, 106, 8035-8046, Doi 10.1029/2000jd900628, 2001.

Stutz, J., Alicke, B., Ackermann, R., Geyer, A., White, A. B., and Williams, E. J.: Vertical profiles of NO_3, N_2O_5, O_3, and NO_x in the nocturnal boundary layer: 1. Observations during the Texas Air Quality Study 2000, Journal of Geophysical Research, 109, 10.1029/2004JD005216, 2004.

Su, L. P., Patton, E. G., de Arellano, J. V. G., Guenther, A. B., Kaser, L., Yuan, B., Xiong, F. L. Z., Shepson, P. B., Zhang, L., Miller, D. O., Brune, W. H., Baumann, K., Edgerton, E., Weinheimer, A., Misztal, P. K., Park, J. H., Goldstein, A. H., Skog, K. M., Keutsch, F. N., and Mak, J. E.: Understanding isoprene photooxidation using observations and modeling over a subtropical forest in the southeastern US, Atmos Chem Phys, 16, 7725-7741, 10.5194/acp-16-7725-2016, 2016.

Suthawaree, J., Kato, S., Pochanart, P., Kanaya, Y., Akimoto, H., Wang, Z. F., and Kajii, Y.: Influence of Beijing outflow on Volatile Organic Compounds (VOC) observed at a mountain site in North China Plain, Atmos Res, 111, 46-57, 10.1016/j.atmosres.2012.02.016, 2012.

Tang, J. H., Chan, L. Y., Chan, C. Y., Li, Y. S., Chang, C. C., Liu, S. C., Wu, D., and Li, Y. D.: Characteristics and diurnal variations of NMHCs at urban, suburban, and rural sites in the Pearl River Delta and a remote site in South China, Atmos Environ, 41, 8620-8632, 10.1016/j.atmosenv.2007.07.029, 2007.

Taraborrelli, D., Lawrence, M. G., Crowley, J. N., Dillon, T. J., Gromov, S., Groß, C. B. M., Vereecken, L., and Lelieveld, J.: Hydroxyl radical buffered by isoprene oxidation over tropical forests, Nat Geosci, 5, 190-193, 10.1038/ngeo1405, 2012.

Vilà-Guerau de Arellano, J., Patton, E. G., Karl, T., van den Dries, K., Barth, M. C., and Orlando, J. J.: The role of boundary layer dynamics on the diurnal evolution of isoprene and the hydroxyl radical over tropical forests, Journal of Geophysical Research, 116, 10.1029/2010jd014857, 2011.

Wang, H. C., Lu, K. D., Tan, Z. F., Sun, K., Li, X., Hu, M., Shao, M., Zeng, L. M., Zhu, T., and Zhang, Y. H.: Model simulation of NO_3, N_2O_5 and $ClNO_2$ at a rural site in Beijing during CAREBeijing-2006, Atmos Res, 196, 97-107, 10.1016/j.atmosres.2017.06.013, 2017.

Wang, M., Zeng, L. M., Lu, S. H., Shao, M., Liu, X. L., Yu, X. N., Chen, W. T., Yuan, B., Zhang, Q., Hu, M., and Zhang, Z. Y.: Development and validation of a cryogen-free automatic gas chromatograph system (GC-MS/FID) for online measurements of volatile organic compounds, Analytical Methods, 6, 9424-9434, 10.1039/c4ay01855a, 2014.

Wang, S., Wang, Y., Zhang, J., Mao, T., and Wang, M.: Observation studies on Changbai mountains area atmospheric VOCs, China Environmental Science, 491-495, 10.3321/j.issn:1000-6923.2008.06.003, 2008.

Wang, T., Guo, H., Blake, D. R., Kwok, Y. H., Simpson, I. J., and Li, Y. S.: Measurements of trace gases in the inflow of South China Sea background air and outflow of regional pollution at Tai O, Southern China, Journal of Atmospheric Chemistry, 52, 295-317, 10.1007/s10874-005-2219-x, 2005.

Wolfe, G. M., Kaiser, J., Hanisco, T. F., Keutsch, F. N., de Gouw, J. A., Gilman, J. B., Graus, M., Hatch, C. D., Holloway, J., Horowitz, L. W., Lee, B. H., Lerner, B. M., Lopez-Hilifiker, F., Mao, J., Marvin, M. R., Peischl, J., Pollack, I. B., Roberts, J.

M., Ryerson, T. B., Thornton, J. A., Veres, P. R., and Warneke, C.: Formaldehyde production from isoprene oxidation across NOx regimes, Atmos Chem Phys, 16, 2597-2610, 10.5194/acp-16-2597-2016, 2016.

Wu, F., Yu, Y., Sun, J., Zhang, J., Wang, J., Tang, G., and Wang, Y.: Characteristics, source apportionment and reactivity of ambient volatile organic compounds at Dinghu Mountain in Guangdong Province, China, The Science of the total environment, 548-549, 347-359, 10.1016/j.scitotenv.2015.11.069, 2016.

Wu, M., Wu, D., Fan, Q., Wang, B. M., Li, H. W., and Fan, S. J.: Observational studies of the meteorological characteristics associated with poor air quality over the Pearl River Delta in China, Atmos Chem Phys, 13, 10755-10766, 10.5194/acp-13-10755-2013, 2013.

Xiao, R., Takegawa, N., Kondo, Y., Miyazaki, Y., Miyakawa, T., Hu, M., Shao, M., Zeng, L. M., Hofzumahaus, A., Holland, F., Lu, K., Sugimoto, N., Zhao, Y., and Zhang, Y. H.: Formation of submicron sulfate and organic aerosols in the outflow from the urban region of the Pearl River Delta in China, Atmos Environ, 43, 3754-3763, 10.1016/j.atmosenv.2009.04.028, 2009.

Xie, X., Shao, M., Liu, Y., Lu, S. H., Chang, C. C., and Chen, Z. M.: Estimate of initial isoprene contribution to ozone formation potential in Beijing, China, Atmos Environ, 42, 6000-6010, 10.1016/j.atmosenv.2008.03.035, 2008.

Xu, L., Guo, H., Boyd, C. M., Klein, M., Bougiatioti, A., Cerully, K. M., Hite, J. R., Isaacman-VanWertz, G., Kreisberg, N. M., Knote, C., Olson, K., Koss, A., Goldstein, A. H., Hering, S. V., de Gouw, J., Baumann, K., Lee, S. H., Nenes, A., Weber, R. J., and Ng, N. L.: Effects of anthropogenic emissions on aerosol formation from isoprene and monoterpenes in the southeastern United States, Proc Natl Acad Sci U S A, 112, 37-42, 10.1073/pnas.1417609112, 2015.

Xue, L. K., Gu, R. R., Wang, T., Wang, X. F., Saunders, S., Blake, D., Louie, P. K. K., Luk, C. W. Y., Simpson, I., Xu, Z., Wang, Z., Gao, Y., Lee, S. C., Mellouki, A., and Wang, W. X.: Oxidative capacity and radical chemistry in the polluted atmosphere of Hong Kong and Pearl River Delta region: analysis of a severe photochemical smog episode, Atmos Chem Phys, 16, 9891-9903, 10.5194/acp-16-9891-2016, 2016.

Yang, Y. D., Shao, M., Kessel, S., Li, Y., Lu, K. D., Lu, S. H., Williams, J., Zhang, Y. H., Zeng, L. M., Noelscher, A. C., Wu, Y. S., Wang, X. M., and Zheng, J. Y.: How the OH reactivity affects the ozone production efficiency: case studies in Beijing and Heshan, China, Atmos Chem Phys, 17, 7127-7142, 10.5194/acp-17-7127-2017, 2017.

Yuan, B., Shao, M., de Gouw, J., Parrish, D. D., Lu, S. H., Wang, M., Zeng, L. M., Zhang, Q., Song, Y., Zhang, J. B., and Hu, M.: Volatile organic compounds (VOCs) in urban air: How chemistry affects the interpretation of positive matrix factorization (PMF) analysis, Journal of Geophysical Research-Atmospheres, 117, 10.1029/2012jd018236, 2012.

Tables

Table 1: Comparison of average concentrations (ppbv) of isoprene, O_3, NO and NO_2 measured at the Nanling site, as well as (MVK+MACR)/isoprene ratios (ppbv/ppbv), with other remote forest sites.

Forest type and latitude	Isoprene	Ratio	O_3	NO	NO_2	Sampling time	References
Subtropical (24.70° N)	0.377	1.9	51.9	0.803	2.386	Daytime (Jul. – Aug.)	This study
	0.159	6.3	55.5	0.656	2.511	Night (Jul. – Aug.)	
Subtropical (23.17° N)	0.760	-	-	-	-	Daytime (All year)	(Wu et al., 2016)
Subtropical (22.29° N)	0.554	-	-	-	-	Daytime (Summer)	(Chen et al., 2010)
Tropical (18.40° N)	0.480	-	-	-	-	Daytime (Apr.)	(Tang et al., 2007)
Deciduous (22.25° N)	0.370	-	30.0	-	-	Daytime (All year)	(Wang et al., 2005)
Temperate (42.40° N)	1.720	-	-	-	-	Daytime (all year)	(Wang et al., 2008)
Tibet (37.59° N)	0.410	-	-	-	-	Daytime (Sep.–Oct.)	(Bai et al., 2016b)
Temperate (45.56° N)	1.360	0.1	-	0.1	1.000	Daily (Summer)	(Apel, 2002)
Tropical (4.98° N)	1.058	0.5	-	-	-	Daily (Apr.–Jul.)	(Jones et al., 2011)
Deciduous (36.21° N)	0.743	0.6	-	-	-	Daily (Jun.–Jul.)	(Link et al., 2015)
Coniferous (38.90° N)	0.397	2.3	-	-	-	Daily (Jun.–Sep.)	(Dreyfus et al., 2002)
Oak (45.20° N)	1.070	0.5	-	-	-	Daily (Jun.–Jul.)	(Acton et al., 2016)
Mediterranean (41.78° N)	0.430	0.7	37.5	0.8	1.000	Daily (Jul.–Aug.)	(Seco et al., 2011)
Tropical (2.59° S)	1.660	-	-	-	-	Daytime (wet season)	(Alves et al., 2016)
Tropical (2.59° S)	3.400	0.31	15.0	-	-	Daytime (dry season)	(Kuhn et al., 2007)

Figures

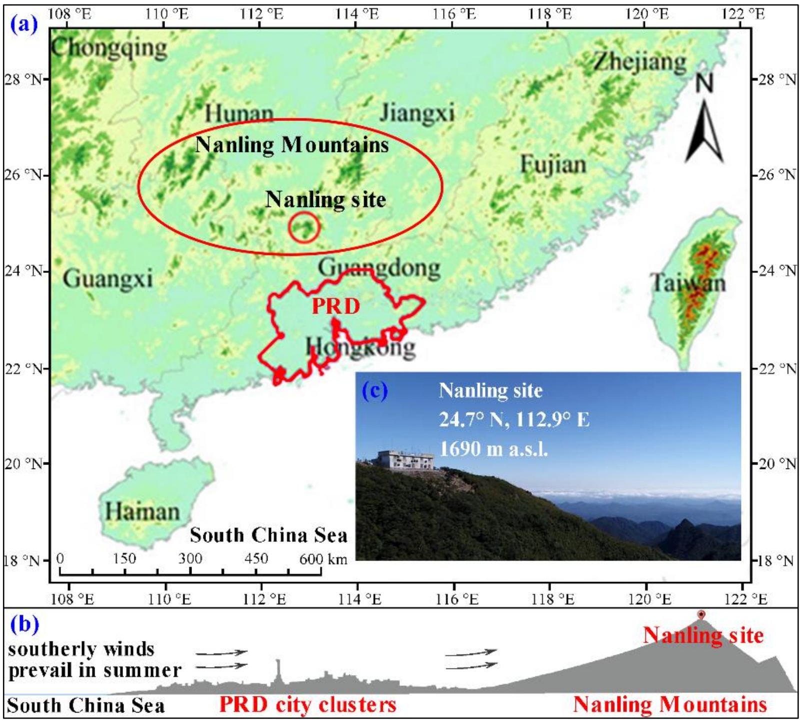

Fig. 1: (a) Map showing the location of the Nanling site at the summit of Mt. Tian Jing in southern Nanling Mountains; (b) Also shown is the sketch of cross section of the PRD and Nanling Mountains; (c) Aerial photo of the Nanling site. The base map in Fig. 1a and Fig.1b is reproduced from Wu et al. (2016) and Wu et al. (2013), respectively.

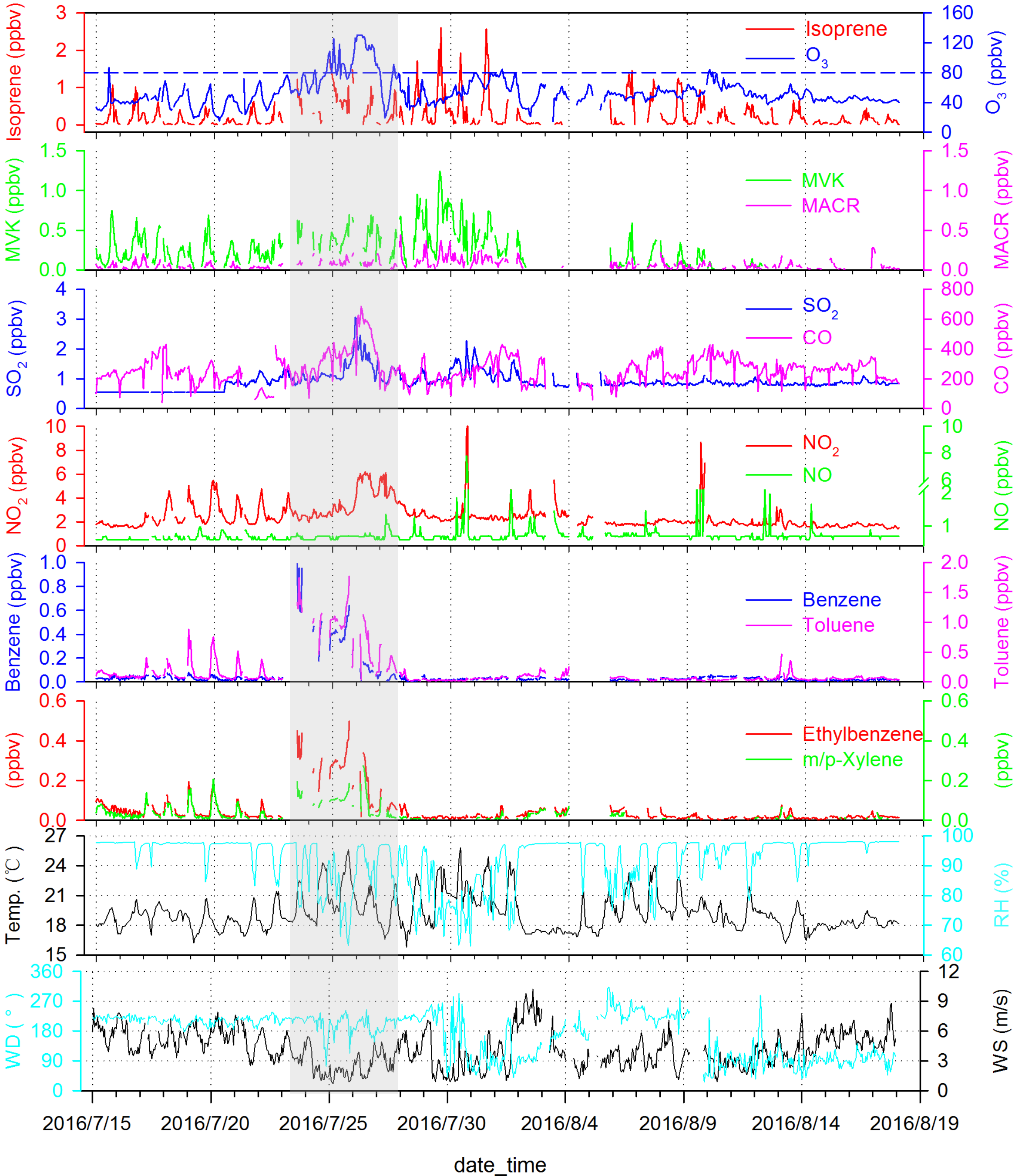

Fig. 2: Time series (1 hour data) of trace gases and meteorological parameters during July–August 2016 at the Nanling site. Blue dashed lines are Grade I of the Ambient Air Quality Standard in China for O_3 (80 ppbv). Temperature, relative humidity, wind speed and wind direction are referred to as Temp., RH, WS and WD, respectively.

Atmos. Chem. Phys. Discuss., https://doi.org/10.5194/acp-2018-336
Manuscript under review for journal Atmos. Chem. Phys.
Discussion started: 16 May 2018

Atmospheric Chemistry and Physics
Open Access
Discussions

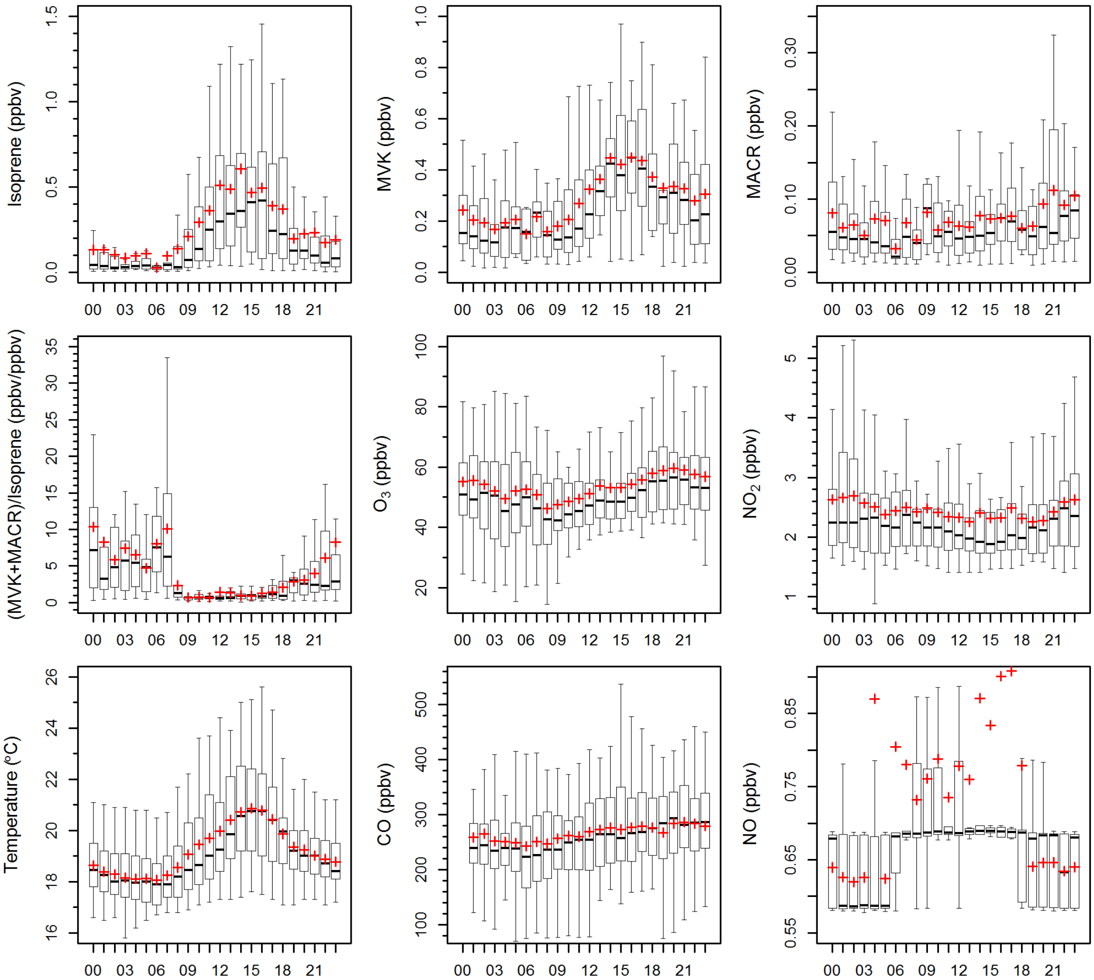

Fig. 3: Box and whisker plots of average diurnal patterns of isoprene, MVK, MACR, (MVK+MACR)/isoprene ratios, O_3, NO_2, temperature, CO and NO. The X-axis is "hour of day". The black thick line and red plus sign represent the median and mean value, respectively.

Atmos. Chem. Phys. Discuss., https://doi.org/10.5194/acp-2018-336
Manuscript under review for journal Atmos. Chem. Phys.
Discussion started: 16 May 2018

Atmospheric Chemistry and Physics
Open Access
Discussions

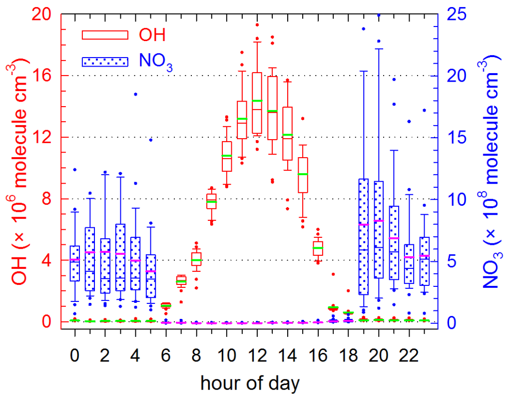

Fig. 4: Box and whisker plots of average diurnal patterns of modeled OH and NO_3 radical. The green and pink thick line represent the mean value.

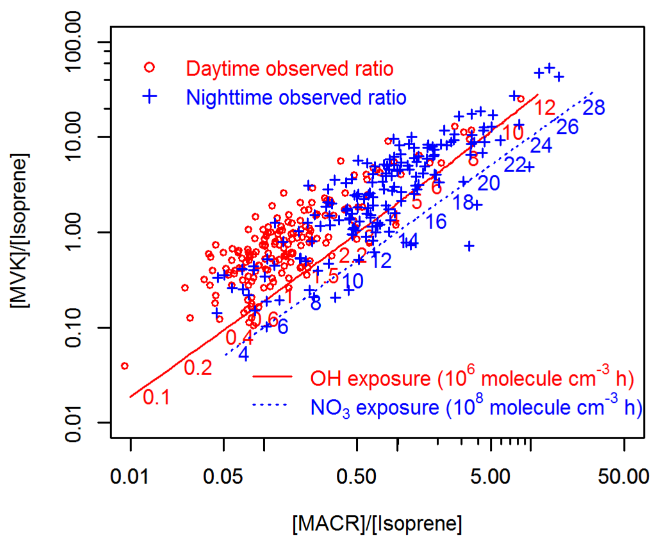

Fig. 5. Isoprene oxidation clock defined by the progression of daughter/parent (MVK/isoprene, MACR/isoprene) ratios (unit: molecules cm^{-3} / molecules cm^{-3}). Red circles and blue crosses show the observed ratios for the daytime and nighttime measurements, respectively. The red solid and blue dashed lines are the results of isoprene sequential reaction scheme calculation. Texts next to the line indicate the theoretical exposures (the product of radical concentration and reaction time) corresponding to any given daughter–parent relationship.

Atmos. Chem. Phys. Discuss., https://doi.org/10.5194/acp-2018-336
Manuscript under review for journal Atmos. Chem. Phys.
Discussion started: 16 May 2018

Atmospheric Chemistry and Physics
Open Access
Discussions

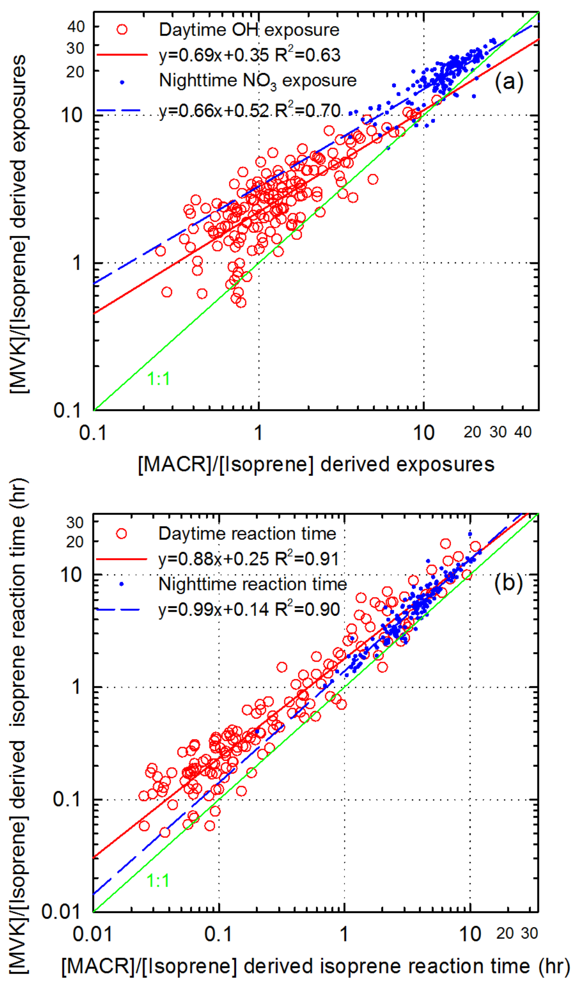

Fig. 6: (a) Scatter plots of exposures derived from observed [MVK]/[isoprene] ratios versus that from [MACR]/[isoprene] ratios. The unit of OH exposure and NO_3 exposure is 10^6 molecules cm^{-3} h and 10^8 molecules cm^{-3} h, respectively. The green line denotes a 1:1 relationship. (b) Isoprene reaction time derived from [MVK]/[isoprene] and [MACR]/[isoprene] method based on the modeled OH and NO_3 concentrations. The green line denotes a 1:1 relationship.

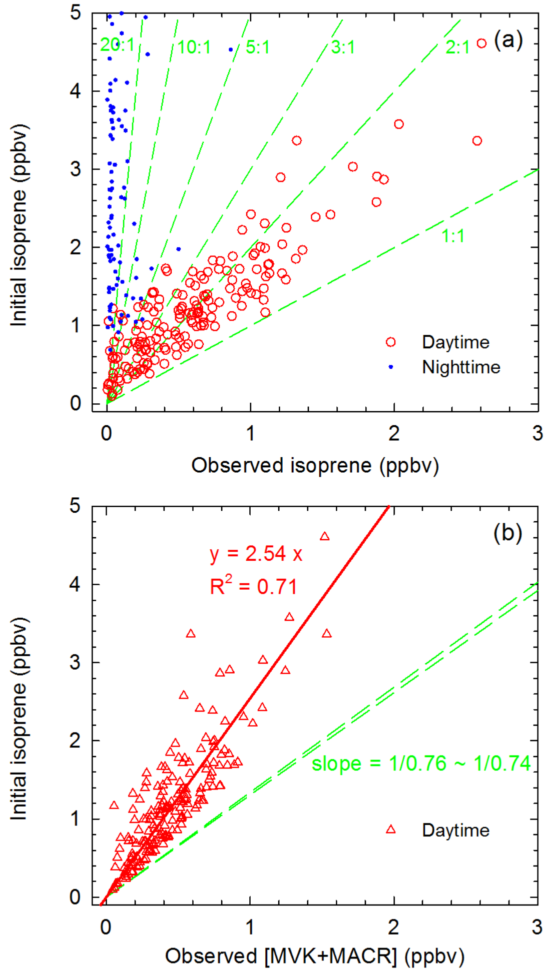

Fig. 7: (a) Comparison of observed and initial isoprene mixing ratios. Green dashed lines denote slopes for different ratios of initial to observed isoprene. (b) Relationship between initial isoprene and measured [MVK+MACR] during the day. The green dashed lines denote slopes for different yields of (MVK+MACR) of the OH-initiated oxidation of isoprene for the ranges of the observed NO distribution (Fig. S1).

Atmos. Chem. Phys. Discuss., https://doi.org/10.5194/acp-2018-336
Manuscript under review for journal Atmos. Chem. Phys.
Discussion started: 16 May 2018

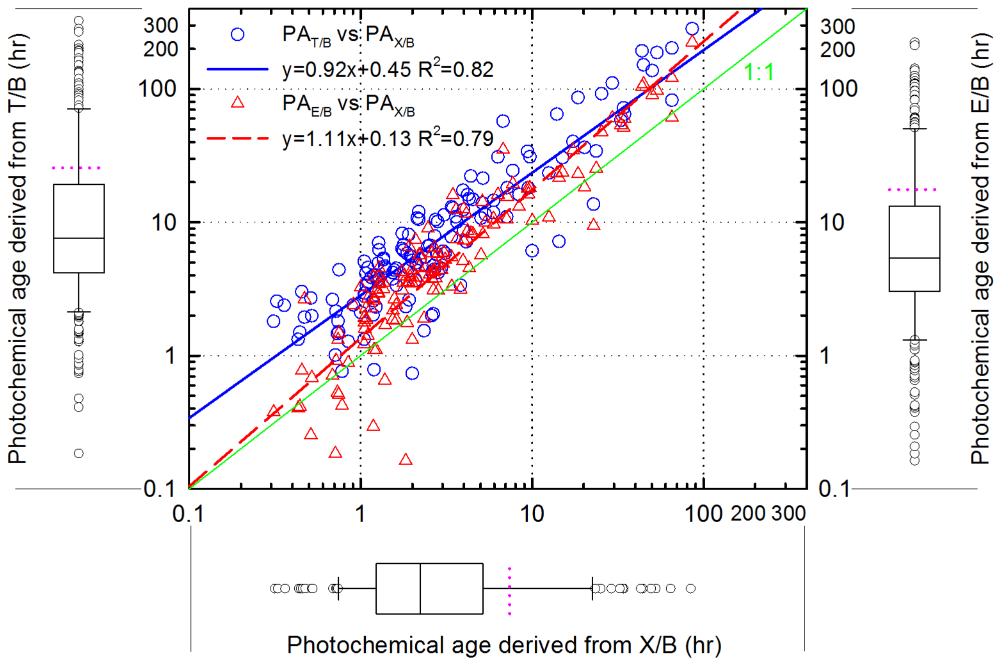

Fig. 8: Photochemical age of the air mass derived from the daytime toluene/benzene (T/B), ethylbenzene/benzene (E/B) and m,p-xylene/benzene (X/B) ratios. The green line denotes a 1:1 relationship. Next to axes are the box and whisker plots of each result, and the pink dotted lines denote the mean values.